Protein Rotational Diffusion and Lipid/Protein Interactions in Recombinants of Bovine Rhodopsin with Saturated Diacylphosphatidylcholines of Different Chain Lengths Studied by Conventional and Saturation-Transfer Electron Spin Resonance

Nicholas J. P. Ryba‡ and Derek Marsh*

Max-Planck-Institut für biophysikalische Chemie, Abteilung Spektroskopie, WD-3400 Göttingen, Federal Republic of Germany

Received February 14, 1992; Revised Manuscript Received May 15, 1992

ABSTRACT: Bovine rhodopsin has been reconstituted in seven different saturated diacylphosphatidylcholine species of odd and even chain lengths from C-12 to C-18 at a lipid/protein ratio (60:1 mol/mol) comparable to that in the native rod outer segment disk membrane. All recombinants were found to be photochemically active, in that optical bleaching produced a temperature- and lipid chain-length-dependent mixture of species absorbing at 480 and 380 nm. Both the rotational diffusion of rhodopsin and lipid–protein interactions in the various recombinants were studied by saturation transfer and conventional electron spin resonance spectroscopy of spin-labeled rhodopsin and of spin-labeled phosphatidylcholine, respectively. In the fluid lipid phase, the rotational diffusion rate of rhodopsin was found to be dependent on the lipid chain length of the different recombinants in a nonmonotonic manner. The diffusion rate in dilauroylphosphatidylcholine was found to be very slow, indicating extensive protein aggregation, whereas that in dipentadecanoylphosphatidylcholine was rapid (effective correlation time ca. 7 μs), consistent with the presence of monomeric protein. For recombinants with longer lipid chain lengths, the rotational diffusion rate again decreased, indicating the presence of di- or oligomeric protein. The fraction of lipid motionally restricted at temperatures in the fluid phase was also dependent on the chain length of the phosphatidylcholine used in the reconstitution. For recombinants with dimyristoyl- and dipentadecanoylphosphatidylcholine, the number of lipids estimated to be associated with the hydrophobic surface of the protein (ca. 22 lipids/protein) was consistent with the presence of monomeric protein of intramembranous diameter of ca. 30 Å. In recombinants with dilauroylphosphatidylcholine, the fraction of motionally restricted lipid was greater, indicating that up to 22 lipids/protein were trapped in the protein aggregates, in addition to those motionally restricted at the hydrophobic perimeter of the protein. For recombinants with phosphatidylcholines of chain lengths longer than C-15, the fraction of motionally restricted lipid was reduced, to a level beyond that of detectability in the case of distearoylphosphatidylcholine. This reduction in hydrophobic surface available to lipids is again consistent with aggregation of the protein in recombinants of longer lipid chain length, indicating extensive protein aggregation for the C-18 chain length. The effects of phospholipid chain length on lipid selectivity at the protein interface are also considered.

Lipid/protein interactions in biological membranes are responsible for preserving the functional integrity of the embedded membrane proteins, in addition to maintaining the membrane permeability barrier. They are governed largely by hydrophobic interactions with the lipid chains and polar interactions with the lipid headgroups. The polar interactions give rise to headgroup selectivity between the different lipid species [for a review, see Marsh (1987)] and modulate the activity of certain membrane-bound enzymes, receptors, or transport proteins. The hydrophobic interactions, on the other hand, are determined to a great extent by a matching of the lipid chain length with the hydrophobic span of the transmembranous sections of the proteins and can have wide-ranging effects on protein stability, function, and aggregation state.

Theoretical models of lipid/protein interactions (Owicki et al., 1978; Jähnig, 1981; Mouritsen & Bloom, 1984) have been advanced which predict a modulation of the lipid phase behavior depending on whether the hydrophobic span of the protein is best matched by the lipid chain length in the gel or in the fluid state. Extremes of mismatch in chain length could lead either to aggregation or to phase separation of the protein. Experimentally, the degree of dispersal of bacteriorhodopsin reconstituted in phosphatidylcholines of different chain lengths has been assessed by freeze fracture electron microscopy (Lewis & Engelman, 1983). It was concluded that the protein mixed well with a range of fluid lipids which have chains of lengths approaching that of dimyristoylphosphatidylcholine (diC_{14}PtdCho).[1] Only when reconstituted in lipids with considerably longer or shorter chain lengths did protein aggregation take place. The state of aggregation of rhodopsin in phosphatidylcholines of different chain lengths has also been studied by rotational diffusion measurements using saturation transfer ESR (Kusumi & Hyde, 1982). In this case it was concluded that a transient, concentration-dependent protein aggregation took place in lipids of chain lengths from C-14 to C-18. Only in the shorter chain-length diC_{12}-PtdCho was static protein aggregation detected.

The rhodopsin system is of considerable interest with regard to possible involvement of lipid/protein interactions in visual transduction. Lipid effects are thought to be important

‡ Present address: National Institute of Dental Research, National Institutes of Health, Building 10/1A09, 9000 Rockville Pike, Bethesda MD 20892.

0006-2960/92/0431-7511$03.00/0

because of the unusually high content of polyunsaturated chains in the native lipids of mammalian ROS disk membranes (Miljanich et al., 1979). On the other hand, little lipid headgroup selectivity is found in interactions with rhodopsin (Watts et al., 1979), suggesting a dominant role for hydrophobic interactions and hence of lipid chain length. Additionally, rhodopsin is known to undergo rapid rotational diffusion in native disk membranes (Cone, 1972), and both this and the aggregation state of the protein might be controlled by the lipid composition of the membrane.

In the present work, we have investigated the rhodopsin system in further detail. Photochemically functional reconstitution was effected in phosphatidylcholines of odd and even chain lengths from C-12 to C-18. The aggregation state of the protein was studied by rotational diffusion measurements using STESR of the spin-labeled protein, and lipid/protein interactions were studied by conventional ESR of spin-labeled phosphatidylcholine. The latter has the advantage that it gives a measure of the hydrophobic perimeter of the protein which is exposed to lipid. The results are interpreted relative to the thermotropic lipid-phase behavior and the thermal stability of the protein in the different reconstituted systems.

MATERIALS AND METHODS

Materials. Spin-labeled maleimide (5-MSL) was obtained from Syva, Palo Alto, CA. Spin-labeled phosphatidylcholine labeled on the C-14 atom of the *sn*-2 chain was synthesized as described in Marsh and Watts (1982). Symmetrical disaturated phosphatidylcholines (1,2-diacyl-*sn*-glycero-3-phosphocholines, diC_nPtdCho) of even chain lengths were from Fluka (Buchs, Switzerland), and those of odd chain lengths were from Avanti (Birmingham, AL).

Rhodopsin Purification and Reconstitution. Bovine rod outer segments were isolated as described in Uhl et al. (1987) and were washed exhaustively in isotonic and then hypotonic buffer to remove peripheral proteins (Kühn, 1980). Rhodopsin solubilized in 60 mM octyl glucoside was purified and delipidated by affinity chromatography over concanavalin-A–Sepharose in 30 mM octyl glucoside (Litman, 1982). Rhodopsin ($A_{280}/A_{500} < 1.7$) was reconstituted in phosphatidylcholine of the required chain length by dialysis from a mixed cholate (15 mM)/octyl glucoside (15 mM) detergent system (Ryba et al., 1986). The lipid/protein recombinants were subjected to isopycnic sucrose density gradient centrifugation, and the sharp rhodopsin-containing band was harvested and washed twice to remove sucrose. All operations were performed in the dark or under dim red light. All buffers used were saturated with argon or nitrogen and, unless otherwise stated, did not contain sulfhydryl reagents. With the exception of column chromatography, all other operations were performed on ice. Phospholipid was determined by phosphate analysis (Eibl & Lands, 1969), and protein according to Markwell et al. (1981).

Sample Preparation. For measurements with spin-labeled phosphatidylcholine, lipid/protein recombinants were doped with 14-PCSL at a level of less than 1 mol % with respect to the total lipid content from a small volume of concentrated spin label in ethanol. The samples were freed from unincorporated label by centrifugation and washing. For STESR measurements, rhodopsin was covalently labeled in recombinants by aqueous reaction with 5-MSL, added in a small volume of ethanol. Recombinants were incubated for 30 min on ice with a 5-fold molar excess of 5-MSL, washed three times, incubated twice on ice with 20 mM dithiothreitol for 30 min, and finally washed a further five times. The spin-labeled sample pellet was packed in a 1-mm-diameter glass capillary by centrifugation and, for STESR measurements, was trimmed in size to 5 mm (Fajer & Marsh, 1982; Hemminga et al., 1984). The buffer used throughout was 5 mM Hepes, 0.1 M NaCl, 1 mM EDTA, pH 7.5, saturated with either argon or nitrogen. All operations were performed in the dark or under dim red light.

Electron Spin Resonance Measurements. ESR spectra were recorded on a Varian Century Line 9 GHz spectrometer equipped with nitrogen gas flow temperature regulation. Spectral recording and sample transfer were performed in the dark or under dim red light. Samples were contained in 1-mm-diameter sealed glass capillaries within a standard 4-mm-diameter quartz tube containing light silicone oil for thermal stability. Temperature was measured by a fine-wire thermocouple situated in the silicone oil at the top of the microwave cavity. Conventional, in-phase, absorption ESR spectra (V_1 display) were recorded at a modulation amplitude of 1.25 G p–p and a modulation frequency of 100 kHz. STESR spectra were recorded in the second harmonic, 90° out-of-phase, absorption mode (V_2' display) at a modulation frequency of 50 kHz and a modulation amplitude of 5 G p–p. For STESR spectra, the microwave power was set for each sample and temperature to give an average microwave field over the sample of $\langle H_1^2 \rangle^{1/2} = 0.25$ G, according to the protocol of Fajer and Marsh (1982). Spectra were stored on a dedicated laboratory computer. Spectral subtractions were performed as described in Ryba et al. (1987); the detailed methodology is given in Marsh (1982). Calibrations of the effective rotational correlation time deduced from the STESR spectra were taken from Horváth and Marsh (1988). The gel-to-fluid lipid phase transition characteristics of the recombinants were recorded by locking the spectrometer field to the central peak in the ESR spectrum of the 14-PCSL label and registering the peak height while continuously scanning the temperature at a rate of 2 °C/min (Marsh & Watts, 1981).

Functional Characterization. The bleaching characteristics of rhodopsin in the different reconstitutions were studied using the polychromatic flash apparatus of Uhl et al. (1984). The sample cuvettes were contained in a thermostated cell block. Bleaching was achieved by exposure of the sample to the measuring light, and a bleaching train was measured by recording a full spectrum at given intervals over a period of 500 ms. More complete details are given in Ryba et al. (1992).

RESULTS

Characterization of Protein/Lipid Recombinants. Rhodopsin was reconstituted in saturated diacylphosphatidylcholines of odd and even chain lengths from C-12 to C-18. The rhodopsin recombinants with the different phosphatidylcholines were obtained as single bands on density gradient

[1] Abbreviations: Rho, bovine rhodopsin; ROS, rod outer segment; diC_{12}PtdCho, 1,2-didodecanoyl-*sn*-glycero-3-phosphocholine; diC_{13}-PtdCho, 1,2-ditridecanoyl-*sn*-glycero-3-phosphocholine; diC_{14}PtdCho, 1,2-ditetradecanoyl-*sn*-glycero-3-phosphocholine; diC_{15}PtdCho, 1,2-dipentadecanoyl-*sn*-glycero-3-phosphocholine; diC_{16}PtdCho, 1,2-dihexadecanoyl-*sn*-glycero-3-phosphocholine; diC_{17}PtdCho, 1,2-diheptadecanoyl-*sn*-glycero-3-phosphocholine; diC_{18}PtdCho, 1,2-dioctadecanoyl-*sn*-glycero-3-phosphocholine; 14-PCSL, 1-acyl-2-[14-(4,4-dimethyloxazolinyl-*N*-oxy)stearoyl]-*sn*-glycero-3-phosphocholine; EDTA, ethylenediaminetetraacetic acid; Hepes *N*-(2-hydroxyethyl)piperazine-*N'*-2-ethanesulfonic acid; 5-MSL, 3-maleimido-2,2,5,5-tetramethyl-1-pyrrolidine-*N*-oxyl; ESR, electron spin resonance; STESR, saturation transfer ESR; V_1, first harmonic ESR absorption signal detected in phase with respect to the field modulation; V_2', second harmonic absorption ESR signal detected 90° out of phase with respect to the field modulation.

Table I: Temperature Limits of the Gel/Fluid Phase Boundaries[a] in Recombinants of Rhodopsin with Saturated Diacylphosphatidylcholines of Different Chain Lengths at a Lipid/Protein Ratio of 60:1 (mol/mol)

lipid	T_g (°C)	T_f (°C)	lipid	T_g (°C)	T_f (°C)
diC_{12}PtdCho	4.0	10.0	diC_{16}PtdCho	33.5	42.0
diC_{13}PtdCho	13.5	20.5	diC_{17}PtdCho	37.0	46.0
diC_{14}PtdCho	16.5	29.5	diC_{18}PtdCho	44.5	53.0
diC_{15}PtdCho	26.5	37.0			

[a] Lower boundary T_g; upper boundary T_f.

Table II: Temperatures of Thermal Bleaching (T_b) for Rhodopsin in Recombinants with Saturated Diacylphosphatidylcholines of Different Chain Lengths at a Lipid/Protein Ratio of 60:1 (mol/mol)

lipid	T_b (°C)	lipid	T_b (°C)
diC_{12}PtdCho	62–70	diC_{16}PtdCho	ca. 70
diC_{13}PtdCho	64.5–72	diC_{17}PtdCho	50–60
diC_{14}PtdCho	68.5–76	diC_{18}PtdCho	53
diC_{15}PtdCho	70–72		

centrifugation. The lipid/protein ratio of the recombinants was ca. 60:1 (mol/mol) in each case. All recombinants were found to be photochemically active in that a temperature-dependent conversion from a 480-nm-absorbing species, characteristic of the metarhodopsin-I photointermediate, to a 380-nm species, characteristic of the metarhodopsin-II intermediate, was observed in each case, after bleaching the 500-nm rhodopsin absorption. The specific bleaching behavior was dependent in a complex fashion on both lipid chain length and phase properties of the protein/lipid recombinants. In general, production of the 380-nm-absorbing species was favored by higher temperatures relative to the gel/fluid lipid phase boundaries. The bleaching results will be reported in detail elsewhere.

The upper and lower temperature limits of the gel-to-fluid lipid phase transition in the various recombinants were determined from continuous temperature scans of the ESR spectra of the 14-PCSL spin label. The temperatures at which the discontinuities occur in the temperature dependence of the lipid mobility are given for the different lipid chain lengths in Table I. The temperatures at which thermal bleaching of rhodopsin occurred in the different recombinants were determined spectrophotometrically. The temperature ranges over which the 500-nm absorption of rhodopsin was lost are given as a function of chain length of the reconstituting lipid in Table II. For the longer lipid chain lengths the denaturation temperatures are appreciably lower than those in native ROS disk membranes [68–76°C; Miljanich et al. (1985)], and for recombinants in diC_{18}PtdCho thermal bleaching takes place immediately on crossing the fluid lipid phase boundary (cf. Table I).

STESR of Spin-Labeled Rhodopsin. Rhodopsin was covalently spin-labeled in the different lipid recombinants by using the maleimide derivative. In general, the conventional ESR spectra indicated a high degree of immobilization of the local motion of the spin label, with very little contamination of the spectrum from labeling of highly mobile groups. The STESR spectra recorded at temperatures in the fluid lipid phase of spin-labeled rhodopsin in recombinants with phosphatidylcholines of different chain lengths are given in Figure 1. The spectra are characteristic of spin labels with different degrees of rotational mobility on the microsecond time scale. The lowest mobility is recorded for the recombinant with the shortest lipid chain length, diC_{12}PtdCho, and the highest mobility for that with intermediate lipid chain length, diC_{15}-

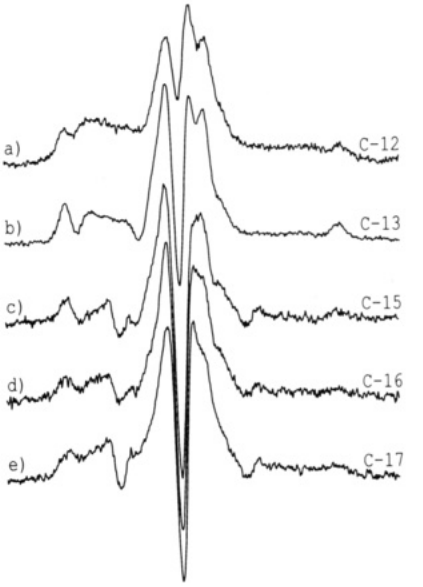

FIGURE 1: Second harmonic, 90° out-of-phase, absorption STESR spectra (V_2' display) of rhodopsin covalently spin-labeled with 5-MSL in recombinants with saturated diacylphosphatidylcholines of different chain lengths at a lipid/protein ratio of 60:1 (mol/mol): (a) Rho/diC_{12}PtdCho at 10 °C; (b) Rho/diC_{13}PtdCho at 25 °C; (c) Rho/diC_{15}PtdCho at 48 °C; (d) Rho/diC_{16}PtdCho at 48 °C; (e) Rho/diC_{17}PtdCho at 53 °C. Total scan width 100 G.

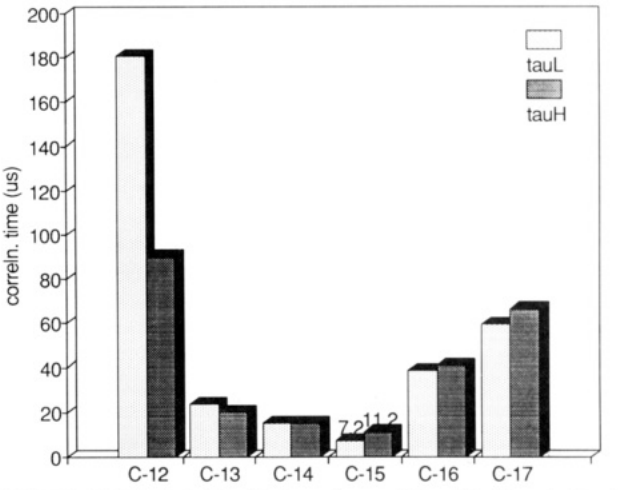

FIGURE 2: Lipid chain-length dependence of the effective rotational correlation times (μs) of 5-MSL-labeled rhodopsin in recombinants with different saturated diacylphosphatidylcholines at a lipid/protein ratio of 60:1 (mol/mol), deduced from the low-field (L''/L, light shading) and high-field (H''/H, heavy shading) line-height ratios in the STESR spectra of Figure 1: C-12, Rho/diC_{12}PtdCho at 10 °C; C-13, Rho/diC_{13}PtdCho at 25 °C; C-14, Rho/diC_{14}PtdCho at 33 °C; C-15, Rho/diC_{15}PtdCho at 48 °C; C-16, Rho/diC_{16}PtdCho at 48 °C; C-17, Rho/diC_{17}PtdCho at 53 °C.

PtdCho. Effective rotational correlation times for the protein in the various recombinants were obtained from the low-field (L''/L) and high-field (H''/H) diagnostic line-height ratios [see Thomas et al. (1976)] by using calibrations from isotropically rotating spin-labeled hemoglobin (Horváth & Marsh, 1988). These values are given as a function of lipid chain length in the recombinant in Figure 2. The longest effective correlation times are obtained with recombinants in diC_{12}PtdCho, with a steep decrease on increasing the lipid chain length, through a minimum at chain lengths of C-14 to C-15, and a subsequent rise on increasing the lipid chain length to diC_{16}PtdCho and diC_{17}PtdCho.

The temperatures chosen for the comparisons in Figures 1 and 2 were taken from the temperature dependences of the

spectra given below to be typical of the protein rotational mobility in the fluid phase. Comparison at a fixed temperature well above the phase transition of all lipids would be less appropriate because of the intrinsic temperature dependences in the fluid phase and the complications with thermal bleaching (cf. Table II) and possible protein denaturation. Strict definition of a reduced temperature is not possible because of the width and different qualitative nature of the phase-separation regions for the lipids of different chain lengths, but the temperatures chosen are approximately representative of such a criterion.

In general, with the exception of diC_{12}PtdCho, the temperature dependence of the STESR spectra of spin-labeled rhodopsin in recombinants with phosphatidylcholines of different chain lengths reflects the chain-melting phase behavior of the lipid. It was found that the spectra are characteristic of a low rotational mobility in the lipid gel phase (e.g., at 4 and 10 °C for diC_{14}PtdCho), an intermediate mobility within the region of the lipid transition at 25 °C (for diC_{14}PtdCho), and a higher mobility in the fluid lipid phase at 33 °C (for diC_{14}PtdCho; data not shown). The temperature dependence of the effective rotational correlation times of the protein deduced from the L''/L and H''/H diagnostic line-height ratios is given for recombinants with phosphatidylcholines of different chain lengths in Figure 3. For reference, the boundaries of the regions of gel and fluid lipid phase separation in the different recombinants are also given in the figure (cf. Table I). The temperature dependence is consistent, as deduced from the two spectral parameters, although the effective correlation times deduced from the L''/L ratio are larger than those deduced from the H''/H ratio, in several cases. The effective rotational correlation times for recombinants with diC_{12}PtdCho remain uniformly high, although all temperatures of measurement are in the fluid lipid phase. In general, the temperature dependences of the effective rotational correlation times in the lipids of chain lengths longer than C-12 correlate with the lipid phase behavior of the different recombinants, in that the rotational rates are slower in the gel-phase lipid at lower temperatures than they are in the fluid-phase lipid at higher temperatures. Exceptions to this are the recombinants with diC_{16}PtdCho and diC_{17}PtdCho, for which the rotational correlation time increases, indicating (partial) protein aggregation on entering the fluid phase.

Conventional ESR of Spin-Labeled Phosphatidylcholine. The different recombinants were doped at a level of ≤1 mol % with phosphatidylcholine (14-PCSL) spin-labeled on the C-14 atom of the *sn*-2 chain. The conventional ESR spectra of 14-PCSL recorded at temperatures in the fluid lipid phase for recombinants with phosphatidylcholines of different chain lengths are given in Figure 4. As is common for lipid/protein systems [cf. Marsh (1985)], the spectra consist of two components: one corresponding to the fluid lipid bilayer regions of the recombinants and the other, with larger hyperfine anisotropy (visible in the outer wings of the spectra), corresponding to the motionally restricted lipid envrionment at the intramembranous surface of the protein. Only in the case of the recombinant with diC_{18}PtdCho is the latter component absent and the spectrum consists entirely of the sharp three-line spectrum characteristic of a fluid lipid bilayer environment. In contrast, the spectrum of the recombinant with diC_{12}PtdCho is dominated by the motionally restricted lipid component. For the other recombinants, the ratio of the intensities of the two spectral components varies less dramatically with chain length.

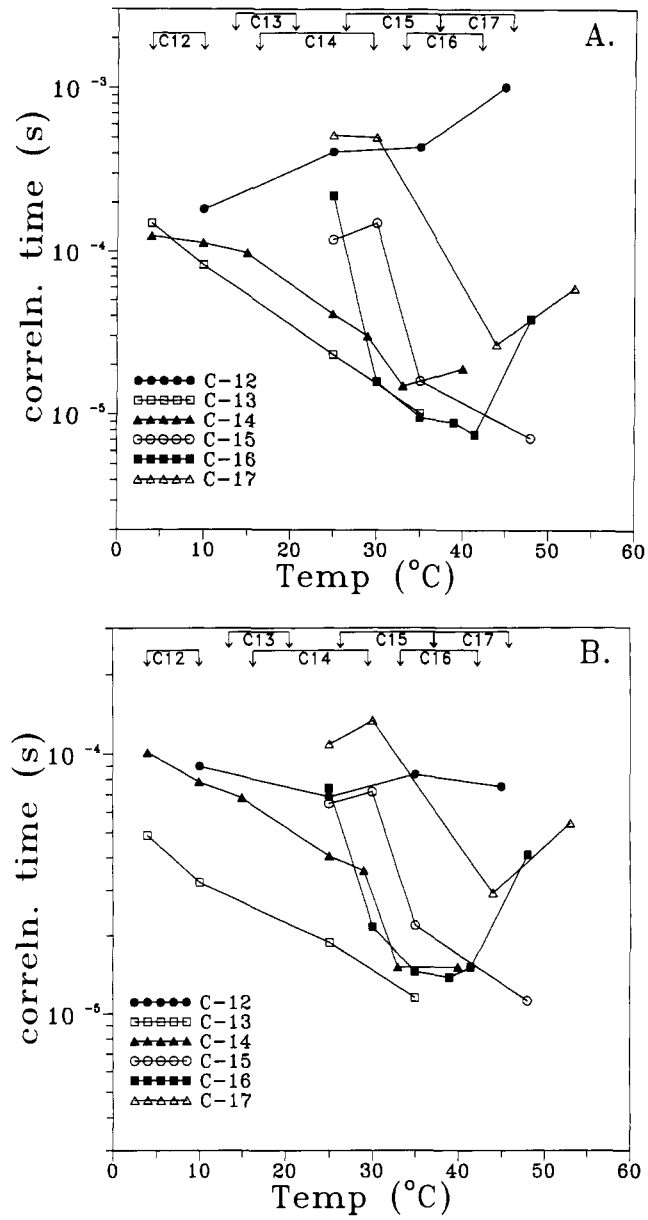

FIGURE 3: Temperature dependence of the effective rotational correlation times of 5-MSL-labeled rhodopsin in recombinants with saturated diacylphosphatidylcholines of different chain lengths at a lipid/protein ratio of 60:1 (mol/mol): (A) values deduced from the low-field (L''/L) line-height ratios in the V_2' STESR spectra; (B) values deduced from the high-field (H''/H) line-height ratios in the V_2' STESR spectra. C-12 Rho/diC_{12}PtdCho; C-13 Rho/diC_{13}PtdCho; C-14 Rho/diC_{14}PtdCho; C-15 Rho/diC_{15}PtdCho; C-16 Rho/diC_{16}PtdCho; C-17 Rho/diC_{17}PtdCho. The temperatures of onset and completion of gel/fluid lipid phase separation for the different recombinants are indicated at the top of each panel (cf. Table I).

The relative proportions of the two components in the spectra of Figure 4 were determined by spectral subtraction and integration as described in Ryba et al. (1987). The fraction of motionally restricted lipid in each of the recombinants with different lipid chain lengths is given in Figure 5. The values obtained for recombinants with diC_{14}PtdCho and with diC_{15}PtdCho are comparable to those found in native ROS disk membranes (Watts et al., 1979; Pates & Marsh, 1987) that have a similar lipid/protein ratio. These values can be taken as representative of the intramembranous surface of the protein that is exposed to lipid. In the recombinant with diC_{12}PtdCho a far greater proportion of the lipid is motionally restricted, correlating with the extensive aggregation in these samples

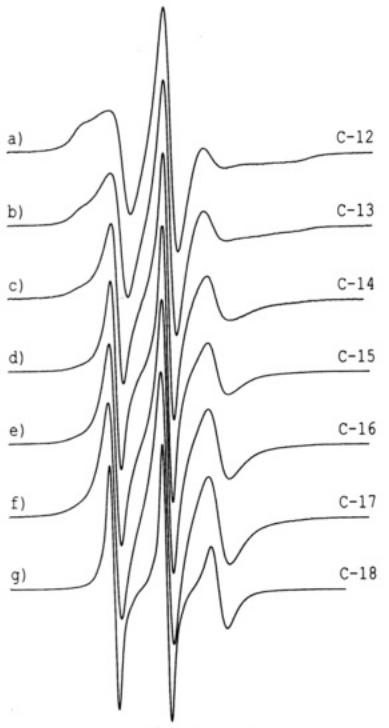

FIGURE 4: Conventional ESR spectra (V_1 display) of spin-labeled phosphatidylcholine (14-PCSL) in recombinants of rhodopsin with saturated diacylphosphatidylcholines of different chain lengths at a lipid/protein ratio of 60:1 (mol/mol): (a) Rho/diC_{12}PtdCho at 20 °C; (b) Rho/diC_{13}PtdCho at 20 °C; (c) Rho/diC_{14}PtdCho at 30 °C; (d) Rho/diC_{15}PtdCho at 40 °C; (e) Rho/diC_{16}PtdCho at 45 °C; (f) Rho/diC_{17}PtdCho at 50 °C; (g) Rho/diC_{18}PtdCho at 54 °C. Total scan width 100 G.

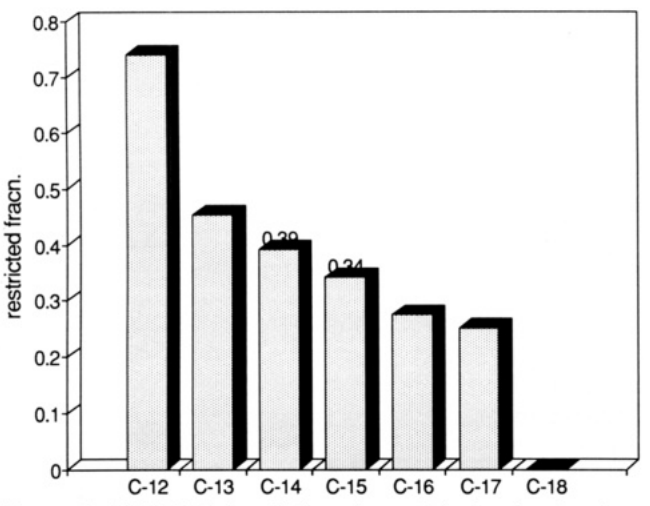

FIGURE 5: Lipid chain-length dependence of the fractional motionally restricted lipid population deduced from the conventional ESR spectra of 14-PCSL in recombinants of rhodopsin with different saturated diacylphosphatidylcholines at a lipid/protein ratio of 60:1 (mol/mol): C-12, Rho/diC_{12}PtdCho at 20 °C; C-13, Rho/diC_{13}PtdCho at 20 °C; C-14, Rho/diC_{14}PtdCho at 30 °C; C-15, Rho/diC_{15}PtdCho at 40 °C; C-16, Rho/diC_{16}PtdCho at 45 °C; C-17, Rho/diC_{17}PtdCho at 50 °C; C-18, Rho/diC_{18}PtdCho at 54 °C.

and suggesting that additional lipid is trapped within the aggregates. At the other extreme, the motionally restricted component in the spectrum of the diC_{18}PtdCho recombinant is beyond the limits of detectability, suggesting extensive protein aggregation with exclusion of lipid from the aggregates.

The temperature dependence of the conventional ESR spectra of 14-PCSL in recombinants of rhodopsin with the phosphatidylcholines of different chain lengths was also investigated. The proportion of motionally restricted lipid

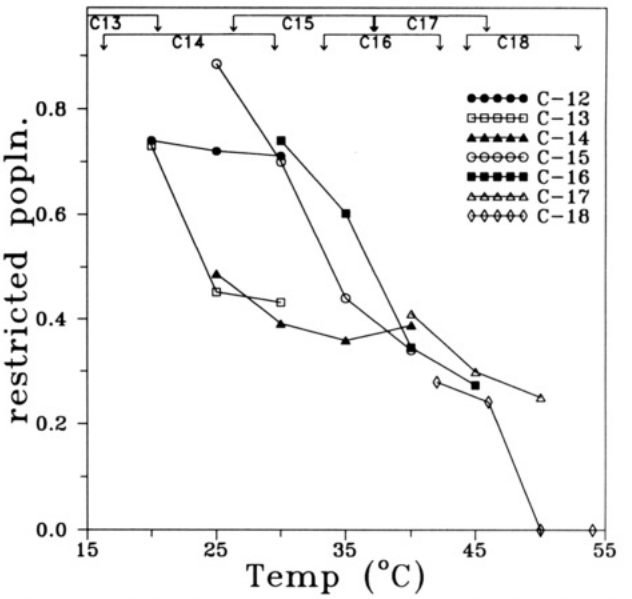

FIGURE 6: Temperature dependence of the fractional motionally restricted lipid population deduced from the conventional ESR spectra of 14-PCSL in recombinants of rhodopsin with saturated diacylphosphatidylcholines of different chain lengths at a lipid/protein ratio of 60:1 (mol/mol): C-12 Rho/diC_{12}PtdCho; C-13 Rho/diC_{13}PtdCho; C-14 Rho/diC_{14}PtdCho; C-15 Rho/diC_{15}PtdCho; C-16 Rho/diC_{16}-PtdCho; C-17 Rho/diC_{17}PtdCho; C-18 Rho/diC_{18}PtdCho. The temperatures of onset and completion of gel/fluid lipid phase separation for the different recombinants are indicated at the top of the figure (cf. Table I).

was found to vary strongly with temperature within the region of gel/fluid lipid phase separation, corresponding to the formation of the less mobile gel-phase lipid. At temperatures above the lipid phase separation region, the motionally restricted component corresponds solely to the lipids interacting directly with the protein. The temperature dependence of the fraction of motionally restricted spin-labeled lipid is given for the recombinants with phosphatidylcholines of different chain lengths in Figure 6. For reference, the boundaries of the regions of gel and fluid lipid phase separation in the different recombinants are also given in the figure (cf. Table I). The fraction of motionally restricted 14-PCSL in recombinants with diC_{12}PtdCho remains uniformly high, although all temperatures of measurement are in the fluid lipid phase. In general, the temperature dependences of the motionally restricted lipid population in the recombinants with lipids of chain lengths longer than C-12 correlate with the lipid phase behavior, in that they increase with increasing population of gel-phase lipid. More significantly, the population remains approximately constant, corresponding to the protein-interacting lipid component, at temperatures in the fluid phase. For recombinants with diC_{18}PtdCho the restricted population is reduced to zero in the fluid lipid phase. This correlates with the spontaneous thermal bleaching of rhodopsin in diC_{18}-PtdCho recombinants immediately on entering the fluid lipid phase (cf. Tables I and II).

DISCUSSION

Photochemically functional recombinants of rhodopsin with diacylphosphatidylcholines of different chain lengths have been prepared and characterized by ESR spectroscopy of spin-labeled rhodopsin and of spin-labeled phosphatidylcholine. Except for recombinants with lipids of the two longest chain lengths, the thermal stability of the protein is comparable to that in ROS disk membranes (Miljanich et al., 1985), with a maximum for the recombinant with diC_{14}PtdCho (see Table

II). Only for the recombinant with the lipid of longest chain length (diC_{18}PtdCho) is the preparation photochemically inactive in the fluid lipid phase due to enhanced thermal bleaching and higher lipid chain melting temperature, T_f (cf. Table I). The effects of the lipid/protein and protein/protein interactions on the optical bleaching behavior are complex and will be reported in detail elsewhere. The purpose here is to use the results obtained from ESR spectroscopy at temperatures in the fluid lipid phase to obtain information about the aggregation state and the nature of the lipid/protein and protein/protein interactions in the recombinants with lipids of different chain lengths. An important feature is the combination of data from reporter groups on the lipid and on the protein in order to determine the detailed nature of the lipid/protein aggregates that give rise to the different thermal sensitivity of the reconstituted rhodopsin.

Protein Rotational Diffusion. The effective rotational correlation time, τ_R^{eff}, deduced from the STESR spectra of spin-labeled rhodopsin can be related to the rotational diffusion coefficient, $D_{R\parallel}$, of the protein aggregate by [see Marsh and Horváth (1989)]:

$$\tau_R^{eff} = 1/(3D_{R\parallel} \sin^2\theta) \quad (1)$$

where θ is the orientation of the spin label z-axis relative to the membrane normal. The rotational diffusion coefficient is related to the cross-sectional dimensions, a and b, and the intramembranous height, h, of the protein aggregate [see Marsh and Horváth (1989)]:

$$D_{R\parallel} = (kT/4\pi\eta a^2 h)F_{R\parallel} \quad (2)$$

where η is the effective intramembranous viscosity and $F_{R\parallel} \leq 1$ is a shape factor which depends only weakly on the asymmetry for small values of a/b (with $a > b$).

Taking the effective rotational correlation time of 7 μs for rhodopsin in diC_{15}PtdCho (Figure 2), together with an interpolated value of h = 40 Å (Tardieu, 1972), and a membrane viscosity of η = 5 P (Cherry & Godfrey, 1981), yields a value of $2a \approx 45$ Å for the effective intramembranous diameter of the protein. This is an upper estimate, since it was assumed that $\theta = 90°$ and $F_{R\parallel} = 1$ in the calculation. The cross-sectional dimensions of the dimer of frog rhodopsin in the low-resolution structure obtained from negatively stained crystals are 22–25 Å × 70–80 Å (Corless et al., 1982), and the radius of gyration determined for bovine rhodopsin is consistent with an elongated cylinder of 31.5-Å diameter or an ellipsoid of 34-Å minor axis (Sardet et al., 1976). Results similar to those for frog rhodopsin have also been obtained from two-dimensional crystals of bovine rhodopsin, although at somewhat lower resolution (Dratz et al., 1985). In view of the uncertainty in the orientation of the spin label axes, the magnitude of the effective correlation time suggests that rhodopsin is present most probably as a monomer in recombinants with diC_{15}PtdCho, as it is in ROS disk membranes (Downer, 1985). In principle, information on the orientation of the spin label axes can be obtained from comparison of the effective correlation times deduced from the central (C'/C) and outer (L''/L or H''/H) line-height ratios (Marsh, 1980). However, the central line-height ratios in the STESR spectra of the recombinants are complicated by the presence of more mobile groups at higher temperatures. Measurements of the C'/C ratios in spin-labeled ROS disk membranes at temperatures for which the contribution from mobile groups can be neglected suggests that $\theta \approx 40°$, which would revise the previous estimate of the intramembranous protein diameter to $2a \approx 29$ Å.

It is clear from eqs 1 and 2 that, if changes in shape factor can be neglected, the effective rotational correlation times are directly proportional to the size of the protein aggregates. For compact aggregates it is likely that $F_{R\parallel} \geq 0.8$, corresponding to $a/b \leq 2$. Effects of the differences in the membrane thickness, h, should give changes in effective rotational correlation time of maximally only ±15%, based on eqs 1 and 2. Thus the values given in Figure 2 can be taken as an indication of the degree of aggregation. In diC_{12}PtdCho there is up to a 25-fold increase in τ_R^{eff} relative to the recombinant in diC_{15}PtdCho, consistent with a high degree of protein aggregation in the former lipid. The present results are in broad agreement with the conclusions of Kusumi and Hyde (1982), although the absolute values of the effective rotational correlation times are somewhat different, possibly because of differences in the reconstitution procedure [compare also Kusumi et al. (1980)]. The rotational diffusion results on protein association can be further augmented by consideration of the lipid/protein interactions in the same systems which are given below.

Lipid/Protein Interactions. The fraction of motionally restricted lipid in recombinants with diC_{14}PtdCho and with diC_{15}PtdCho is ca. 0.36, corresponding to approximately 22 lipids/protein. This number is similar to that determined in native ROS disk membranes (Watts et al., 1979; Pates et al., 1985; Pates & Marsh, 1987). The assumption that the motionally restricted lipids are accommodated around the intramembranous perimeter of the protein (cf. Marsh, 1985), and taking the diameter of a lipid chain as 5 Å, would require an effective protein diameter of ca. 30 Å. This is in accord with the dimensions of the rhodopsin molecule quoted above and further suggests that the protein is present in monomeric form in diC_{14}PtdCho and in diC_{15}PtdCho, as in native ROS disk membranes (Cone, 1972; Downer, 1985). It will also be noted that randomly distributed intramembranous particles are observed by freeze fracture electron microscopy on quenching recombinants with diC_{14}PtdCho from temperatures above the transition region (Chen & Hubbell, 1973).

The gradual change in the fraction, f, of motionally restricted phosphatidylcholine spin label with lipid chain length in rhodopsin recombinants with diC_{13}PtdCho to diC_{17}PtdCho (see Figure 5) possibly could be the result of limited changes in the hydrophobic surface of rhodopsin accessible to lipid, arising from a limited degree of aggregation of the protein (see further below). Alternatively, these changes might indicate differences in affinity for rhodopsin of the fixed chain-length spin label relative to the different chain-length host lipids, diC_nPtdCho. In the latter case, the association constant of the spin-labeled lipid with rhodopsin, relative to that of the background host lipid, is given by (Marsh, 1985)

$$K_r = (n_t/N_1 - 1)f/(1 - f) \quad (3)$$

where n_t is the lipid/protein ratio in the recombinant and N_1 is the number of first-shell lipid association sites on the protein. The free energy of association of the spin label in the different recombinants is given by $\Delta G = -RT \ln K_r$, and hence from eq 3, the chain-length dependence is given by the expression $-RT \ln (f/1-f)$, where it is assumed that N_1 remains constant. From Figure 7 it is seen that this quantity is approximately linearly dependent on chain length, consistent with a competition between the spin-labeled lipid and the host lipids of different chain lengths over the range n = 13 to n = 17. The gradient with respect to chain length of the apparent free energy of association in Figure 7 is approximately $0.25RT$ per CH_2 group. This value is considerably smaller than the

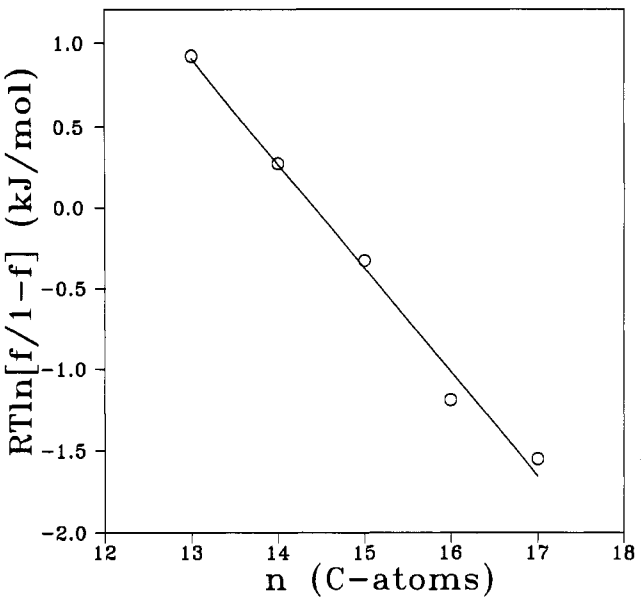

FIGURE 7: Chain-length dependence of the apparent free energy of association, $RT \ln (f/1-f)$, of the 14-PCSL phosphatidylcholine spin label with rhodopsin in recombinants with different phosphatidylcholines, $diC_nPtdCho$, at a lipid/protein ratio of 60:1 (mol/mol). The zero level corresponds to $K_r = 1$ and $N_1 = 22$ in eq 3. The line is a linear regression over the range $n = 13$ to $n = 17$.

free energy of transfer of phosphatidylcholines from water to bilayers [see, for example, Cevc and Marsh (1989)], as would be expected since the present case the spin label is transferred from the bilayer phase to the lipid/protein interface, both of which environments are hydrophobic.[2] Extrapolation of the linear chain-length dependence in Figure 7 to the extreme chain lengths predicts a value of $f = 0.52$ for $diC_{12}PtdCho$ and $f = 0.20$ for $diC_{18}PtdCho$. Both of these values are very different from those measured experimentally (see Figure 5), suggesting that some mechanism other than competition at the lipid/protein interface is responsible for the large departures in the measured values of f for the recombinants with lipids of the extreme chain lengths. This is almost certainly the effect of protein aggregation.

Since the evidence from STESR demonstrates that the protein is strongly aggregated in recombinants with diC_{12}-PtdCho, the increased proportion of motionally restricted lipid found in the latter relative to recombinants with $diC_{14}PtdCho$ or $diC_{15}PtdCho$ indicates that additional lipids must be motionally restricted by being trapped within the protein aggregates. Such a conclusion would be consistent with freeze fracture electron microscopy results (Chen & Hubbell, 1973) which revealed intramembranous particles that were dispersed but with a tendency to associate in dark-adapted recombinants with $diC_{12}PtdCho$. The large population of motionally restricted lipids observed with the $diC_{12}PtdCho$ recombinants corresponds approximately to an additional 22 lipids per protein monomer that are more directly perturbed by the lipid/protein interaction. This value is reduced to 12 lipids/protein if correction is made for a possible chain-length selectivity, based on linear extrapolation in Figure 7.

The protein aggregation that takes place in recombinants with the lipids of longer chain lengths clearly has a different effect on the lipid/protein interaction. Rather than trapping lipids, the protein interface exposed to lipid is reduced by protein/protein interaction. In the case of recombinants with $diC_{16}PtdCho$ or $diC_{17}PtdCho$, the degree of aggregation and of lipid exclusion, if any, is limited. If the possible chain-length selectivity discussed above is ignored, the observed reduction in the fraction of motionally restricted lipid for diC_{17}-PtdCho recombinants would be consistent with dimer or trimer formation. For recombinants with $diC_{18}PtdCho$, the extent of aggregation is more extensive; the large reduction in the fraction of motionally restricted lipid is much greater than can be accounted for by extrapolation of the chain-length dependence of the lipid selectivity in Figure 7. Lipid is excluded from the protein aggregates in recombinants with $diC_{18}PtdCho$, and the hydrophobic surface presented by rhodopsin to the lipid is much smaller. This is consistent with the fact that the aggregation of rhodopsin in $diC_{18}PtdCho$ arises from thermal denaturation of the protein, whereas that in $diC_{12}PtdCho$ still leaves the protein photochemically active.

In summary, the study of the lipid/protein interactions provides additional information on the nature of the protein aggregation processes observed by rotational diffusion measurements with saturation transfer ESR and also provides insight into the selectivity of interaction of rhodopsin with lipids of different chain length.

[2] The analysis embodied in Figure 7 is consistent generally with any thermodynamic mechanism where the free energy of interaction with rhodopsin is linearly dependent on the lipid chain length. Of these, the hydrophobic interaction is a likely candidate, but others such as the van der Waals interaction are also possible. It will be noted also that, in the lipids of different chain length, the spin label group may be located at different positions relative to the hydrophobic span of the protein and possibly also relative to the bilayer surface. In the latter case, the spin label will experience a different region of the motional gradient in the bilayer core, although this effect will be somewhat masked by the different temperatures of measurement. It is unlikely that these latter effects will give rise to the changes in the fraction of motionally restricted lipid shown in Figure 5. On the one hand, little or no selectivity of 14-PCSL is observed relative to unlabeled $diC_{14}PtdCho$ in the interaction with rhodopsin (Ryba et al., 1987); on the other hand no selectivity is found between lipids labeled at different positions down the chain (Pates & Marsh, 1987).

REFERENCES

Chen, Y. S., & Hubbell, W. L. (1973) *Exp. Eye Res. 17*, 517–532.

Cherry, R. J., & Godfrey, R. E. (1981) *Biophys. J. 36*, 257–276.

Cone, R. A. (1972) *Nature (New Biol.) 236*, 39–43.

Corless, J. M., McCaslin, D. R., & Scott, B. R. (1982) *Proc. Natl. Acad. Sci. U.S.A. 79*, 1116–1120.

Downer, N. W. (1985) *Biophys. J. 47*, 285–293.

Dratz, E. A., Van Breemen, J. F. L., Kamps, K. M. P., Keegstra, W., & Van Bruggen, E. F. J. (1985) *Biochim. Biophys. Acta 832*, 337–342.

Eibl, H., & Lands, W. E. M. (1969) *Anal. Biochem. 30*, 51–57.

Fajer, P., & Marsh, D. (1982) *J. Magn. Reson. 49*, 212–224.

Hemminga, M. A., de Jager, P. A., Marsh, D., & Fajer, P. (1984) *J. Magn. Reson. 59*, 160–163.

Horváth, L. I., & Marsh, D. (1988) *J. Magn. Reson. 80*, 314–317.

Jähnig, F. (1981) *Biophys. J. 36*, 329–345.

Kühn, H. (1980) *Nature (London) 283*, 587–589.

Kusumi, A., & Hyde, J. S. (1982) *Biochemistry 21*, 5978–5983.

Kusumi, A., Sakaki, T., Yoshizawa, T., & Ohnishi, S. (1980) *J. Biochem. 88*, 1103–1111.

Lewis, B. A., & Engelman, D. M. (1983) *J. Mol. Biol. 166*, 203–210.

Litman, B. J. (1982) *Methods Enzymol. 81*, 150–153.

Markwell, M. A. K., Haas, S. H., Tolbert, N. E., & Bieber, L. L. (1981) *Methods Enzymol. 72*, 296–303.

Marsh, D. (1980) *Biochemistry 19*, 1632–1637.

Marsh, D. (1982) *Tech. Life Sci.: Biochem. B4*, B426/1–B426/44.

Marsh, D. (1985) in *Progress in Protein–Lipid Interactions* (Watts, A., & De Pont, J. J. H. H. M., Eds.) Vol. 1, pp 143–172, Elsevier, Amsterdam.

Marsh, D. (1987) *J. Bioenerg. Biomembr. 19*, 677–689.

Marsh, D., & Watts, A. (1981) in *Liposomes: From Physical Properties to Therapeutic Applications* (Knight, C. G., Ed.) pp 139–188, Elsevier/North-Holland, Amsterdam, New York, and Oxford.

Marsh, D., & Watts, A. (1982) in *Lipid–Protein Interactions* (Jost, P. C., & Griffith, O. H., Eds.) Vol. II, pp 53–126, Wiley-Interscience, New York.

Marsh, D., & Horváth, L. I. (1989) in *Advanced EPR. Applications in Biology and Biochemistry* (Hoff, A. J., Ed.) pp 707–752, Elsevier, Amsterdam.

Miljanich, G. P., Sklar, L. A., White, D. L., & Dratz, E. A. (1979) *Biochim. Biophys. Acta 552*, 294–306.

Miljanich, G. P., Brown, M. F., Mabrey-Gaud, S., Dratz, E. A., & Sturtevant, J. M. (1985) *J. Membr. Biol. 85*, 79–86.

Mouritsen, O. G., & Bloom, M. (1984) *Biophys. J. 46*, 141–153.

Owicki, J. C., Springgate, M. W., & McConnell, H. M. (1978) *Proc. Natl. Acad. Sci. U.S.A. 75*, 1616–1619.

Pates, R. D., & Marsh, D. (1987) *Biochemistry 26*, 29–39.

Pates, R. D., Watts, A., Uhl, R., & Marsh, D. (1985) *Biochim. Biophys. Acta 814*, 389–397.

Ryba, N. J. P., Dempsey, C. E., & Watts, A. (1986) *Biochemistry 25*, 4818–4825.

Ryba, N. J. P., Horváth, L. I., Watts, A., & Marsh, D. (1987) *Biochemistry 26*, 3234–3240.

Ryba, N. J. P., Marsh, D., & Uhl, R. (1992) (submitted for publication).

Sardet, C., Tardieu, A., & Luzzati, V. (1976) *J. Mol. Biol. 105*, 383–407.

Tardieu, A. (1972) Thesis, Doctorat d'Etat, Université de Paris-Sud.

Thomas, D. D., Dalton, L. R., & Hyde, J. S. (1976) *J. Chem. Phys. 65*, 3006–3024.

Uhl, R., Desel, H., & Wagner, R. (1984) *J. Biochem. Biophys. Methods 10*, 35–48.

Uhl, R., Desel, H., Ryba, N. J. P., & Wagner, R. (1987) *J. Biochem. Biophys. Methods 10*, 35–48.

Watts, A., Volotovski, I. D., & Marsh, D. (1979) *Biochemistry 18*, 5006–5013.